scientific reports

OPEN

Aberrant dynamic functional network connectivity in patients with diffuse axonal injury

Jian Li[1,2,4], Yao Wang[1,2,4], Yuanyuan Wang[1,2], Jie Zhan[1,2], Weiming Sun[3], Feng Ouyang[1,2], Xiumei Zheng[1,2], Lianjiang Lv[1,2], Zihe Xu[1,2], Jie Liu[1,2], Fuqing Zhou[1,2] & Xianjun Zeng[1,2✉]

Diffuse axonal injury (DAI) results in aberrant functional connectivity and is significantly linked to cognitive impairment. Nevertheless, the network mechanisms influencing neurocognitive function following DAI remain unclear. This study aimed to examine the characteristics of static and dynamic functional network connectivity (FNC) in patients with DAI. Resting-state functional magnetic resonance imaging data were collected from 26 patients with DAI and 27 healthy controls. Resting-state networks were extracted using independent component analysis. We evaluated the connectivity strength through spatial maps and static FNC, and then further dynamic properties were identified using a sliding time-window approach and k-means clustering, and investigated their associations with clinical variables. Patients with DAI showed stronger intra-network spatial maps in the default mode network and subcortical network than healthy controls, but static inter-network functional connectivity remained stable. Furthermore, three recurring states for dynamic connectivity were identified in all participants, and state 1 occurred most frequently in patients with DAI and exhibited higher fractional time, and as well as longer mean dwell time, which was positively associated with MMSE scores. Meanwhile, patients with DAI exhibited mostly increased functional connectivity strength of dynamic FNC in all states, particularly within the default mode network and visual network. These findings suggest that patients with DAI are characterized by altered dynamic FNC and temporal properties, which provide distinct complementary information different from static functional connectivity, and new insights into the neural pathophysiology of DAI associated with cognitive impairment.

Traumatic brain injury (TBI) is characterized by remarkable heterogeneity, variable progression, and persistent symptoms. An estimated 69 million patients are affected by TBI annually, constituting a significant cause of death and disability worldwide[1]. Diffuse axonal injury (DAI) is a relatively severe pathological TBI type that may disrupt the functional coordination of large-scale brain networks, and plays a significant role in causing cognitive, behavioral, and affective deficits in patients with TBI[2]. DAI patterns are generally widespread in TBI and highly variable among individuals owing to varying symptoms and unclear progressive mechanisms[3,4], which may have complex effects on brain functional connectivity (FC) after TBI. Advancements in neuroimaging techniques have significantly enhanced our understanding of the underlying pathophysiology of cognitive impairment following TBI[2,5–7]. Altered static FC in different brain regions and network connectivity have emerged as promising biomarkers of cognitive impairment after TBI in various studies[8–10]. However, the heterogeneity of patients with TBI has resulted in varied comprehension of the correlation between cognitive impairment and brain FC in prior studies[11], and primarily involved individuals with mild TBI and not in moderate to severe TBI patients. The pathophysiological mechanism of cognitive function deficits in patients with pure DAI remains uncertain.

Resting-state functional magnetic resonance imaging (rs-fMRI) has emerged as a reliable imaging technique for visualizing brain activity and quantifying distinct FC patterns[12,13]. Multiple previous studies have demonstrated that cognitive impairment after TBI were associated with alterations in disrupted FC in several

[1]Department of Radiology, The First Affiliated Hospital, Jiangxi Medical College, Nanchang University, Nanchang, Jiangxi, People's Republic of China. [2]Clinical Research Center for Medical Imaging in Jiangxi Province, Nanchang, People's Republic of China. [3]Rehabilitation Department, The First Affiliated Hospital, Jiangxi Medical College, Nanchang University, Nanchang, People's Republic of China. [4]These authors contributed equally: Jian Li and Yao Wang. ✉email: xianjun-zeng@126.com

brain regions with inconsistent results, including hyper- and hypoconnectivity[9,10,14–16]. Moreover, resting-state networks (RSNs) can be observed using rs-fMRI and assessed to examine potential abnormalities within and between different networks[2]. Recent studies have indicated that widespread functional network connectivity (FNC) impairments and altered integration occur in TBI patients[2,17]. Numerous studies have revealed aberrant FC patterns within networks such as the default mode network (DMN), executive control network (ECN), salience network, and visual network (VIS) in individuals with TBI[6,18]. Meanwhile, altered FNC in inter-network such as the DMN-attention network and VIS-attention network[9], as well as the cerebellum network (CN)-SMN[19], have been identified in previous mild TBI studies. These results suggest that TBI disrupts coordinated relationships within large-scale functional brain networks and internetworks, reflecting clinically relevant phenomena.

Nevertheless, a multitude of previous neuroimaging studies have regarded the BOLD signal as intrinsically static, assuming that the FC remains constant throughout the entire recording period, ignoring the important dynamic aspect over time[9,20]. Dynamic FC introduces an additional dimension to rs-fMRI analysis and delivers distinct insights into FC that cannot be obtained using conventional static rs-fMRI techniques[21], potentially serving as more sensitive indicators of macro-level changes in neural activity than static FC[22–24]. By elucidating the temporal dynamics of the brain and characterizing variations in functional organization and interregional cooperation, dynamic FNC (dFNC) analysis has been increasingly utilized and unveiled insights into the pathogenesis of certain diseases, such as post-traumatic headache[17], Parkinson's disease[25], neuromyelitis optica spectrum disorders[26], schizophrenia and autism[27]. Studies on mild TBI have demonstrated the potential utility of dFNC as a biomarker, emphasizing its clinical relevance in cognitive impairment[28,29]. Compared to controls, mild TBI patients demonstrated significantly increased and more variable dynamic cross-network interactions associated with cognitive and behavioral outcomes[30]. The combination of static FNC (sFNC) and dFNC methods has the potential to capture complementary information as neuroimaging biomarkers in patients with mild TBI[31,32]. However, alterations of sFNC and dFNC levels in patients with pure DAI (moderate to severe TBI) and their correlation with cognitive impairment remain largely unknown.

Therefore, the current study aimed to investigate abnormalities in sFNC and dFNC at the whole-brain level between patients with DAI and healthy controls (HCs). RSNs were identified using independent component analysis (ICA). We evaluated the connectivity strength through spatial maps (SMs) and sFNC, and then further dynamic properties were identified using a sliding time-window approach and k-means clustering. Correlation analyses between sFNC and dFNC abnormalities and clinical scale scores were performed in patients with DAI. We hypothesized that changes in dFNC and the temporal properties of dynamic FC states could serve as sensitive indicators for characterizing the underlying nature of patients with DAI.

Materials and methods
Study subjects
Between April 2013 and December 2017, the Department of Neurosurgery of the First Affiliated Hospital of Nanchang University recruited 182 patients with TBI, from whom 26 with DAI were selected retrospectively. The inclusion criteria for patients with DAI were as follows: (1) presence of typical closed craniocerebral injury with rapid acceleration-deceleration or high-speed rotation; (2) moderate-severe brain injury with loss of consciousness of 30 min or more; (3) presence of related clinical manifestations of DAI and characterized by microbleed lesions on the magnetic susceptibility sequence; and (4) being right-handed and aged 18–60 years. The exclusion criteria for screening were as follows: (1) having a preexisting TBI history, cerebrovascular disease, or neurological disorders; (2) presence of other forms of TBI diagnosis, including significant cerebral hemorrhage, cerebral contusion, and subdural or epidural hematoma (volume > 10 mL) on computed tomography and MRI; and (3) inability to complete or perform an MRI examination. Twenty-seven healthy volunteers were recruited as HCs from the local community through advertisements without neurological or psychiatric disorders, prior TBI, or other brain diseases.

Each patient with DAI was assessed using a detailed clinical interview and physical examination within 2 h before the MRI scans, including (1) the Glasgow Coma Score (GCS) for assessment of consciousness level impairment and brain injury severity; (2) the Activities of Daily Living and Motor Assessment Scale to assess the essential abilities needed for independent self-care or everyday motor functions; (3) the Disability Rating Scale to assess the level of disability and rehabilitation; (4) the Chinese version of the Mini-Mental State Examination (MMSE) for the swift evaluation of an individual's cognitive function; and (5) the Agitated Behavior Scale and Hamilton Anxiety Scale to identify unhealthy mood and gauge its severity.

This study adhered to the Declaration of Helsinki and was approved by the Medical Ethics Committee of the First Affiliated Hospital of Nanchang University All participants and/or their family members provided informed consent and signed informed consent forms before the examination.

MR data acquisition
Resting-state functional MRI data were acquired using a 3 T MRI system (Trio, Siemens, Munich, Germany) equipped with an eight-channel, phased-array head coil, and data acquisition was performed using a scanning GRE-EPI sequence. The specific parameters for the MRI scan included a repetition time (TR) of 2000 ms, echo time (TE) of 30 ms, field of view (FOV) of 200×200, matrix size of 64×64, flip angle of 90°, and layer thickness of 4 mm. The scan encompassed a continuous acquisition of 30 layers, spanning a total duration of 8 min, and comprising 240 volumes. During the scanning process, the patients were instructed to maintain silence, relax their thoughts, breathe calmly, and keep their eyes closed while awake. Sagittal 3D-T1WI was conducted using the following specific parameters: TR, 1900 ms; TE, 2.26 ms, voxel size, 1 mm × 1 mm × 1 mm; matrix, 256×256; and 176 acquired slices. All participants underwent magnetic susceptibility-weighted imaging with the following parameters: TR, 28 ms; TE, 20 ms; FOV, 240×240, matrix size, 448×384; flip angle, 15°; and

bandwidth, 15.6 kHz and 1.2 mm. Additionally, computed tomography and conventional MRI were performed to rule out brain disease.

Data preprocessing

Data preparation for this study utilized the Data Processing and Analysis of Brain Imaging (DPABI v6.0, https://www.rfmri.org/dpabi) based on the Statistical Parametric Mapping (SPM12 v7219, https://www.fil.ion.ucl.ac.uk/spm/software/spm12/) toolkit on the MATLAB 2016b platform (The MathWorks, Inc., Natick, MA, USA). The following specific steps were taken: the initial 10 volumes of resting-state fMRI data were excluded, and in evaluating head movement realignment, we assessed the mean framewise displacement (FD) for each subject to indicate the average head movement. Images with head motion translation of > 2 mm or rotation by > 2° during functional imaging were excluded. The spatial normalization into the Montreal Neurological Institute (MNI) space and subsequent resampling were performed with $3 \times 3 \times 3$ mm^3. Spatial smoothing was performed using a 6 mm full-width half-maximum Gaussian kernel to enhance the signal-to-noise ratio.

Group independent component analysis

After data preprocessing, the spatial ICA method, implemented by the Group ICA of fMRI Toolbox (GIFT v3.0b, http://mialab.mrn.org/software/gift) was used to analyze the data of all subjects. The dimensionality of the rs-fMRI data was decreased using principal component analysis. Subsequently, the components were estimated using the Infomax ICA algorithm, which identified 30 components. To ensure the stability of the estimate, the ICA components underwent 100 iterations using the ICASSO algorithm (v1.21, http://www.cis.hut.fi/projects/ica/icasso), and the process was repeated five times to select the independent components with an average intra-cluster similarity value exceeding 80%. According to a prior study[33,34], independent components were selected based on the following criteria: (1) the peak coordinates of the components are mainly located in the gray matter; (2) components located in the brain white matter, ventricles, and brainstem are excluded; (3) the components have a high dynamic range (i.e., the difference between the highest and lowest power on the right side of the average power spectrum of the components must be > 0.025); (4) the condition of low to high frequency power ratio being > 3 is satisfied (i.e., the ratio of the spectral power below 0.0667 Hz to the spectral power between 0.01 and 0.1667 Hz is > 4). Subsequently, a visual inspection was conducted, and a total of 20 components were identified. Figure 1 displays schematic illustration of the functional network analyses pipeline.
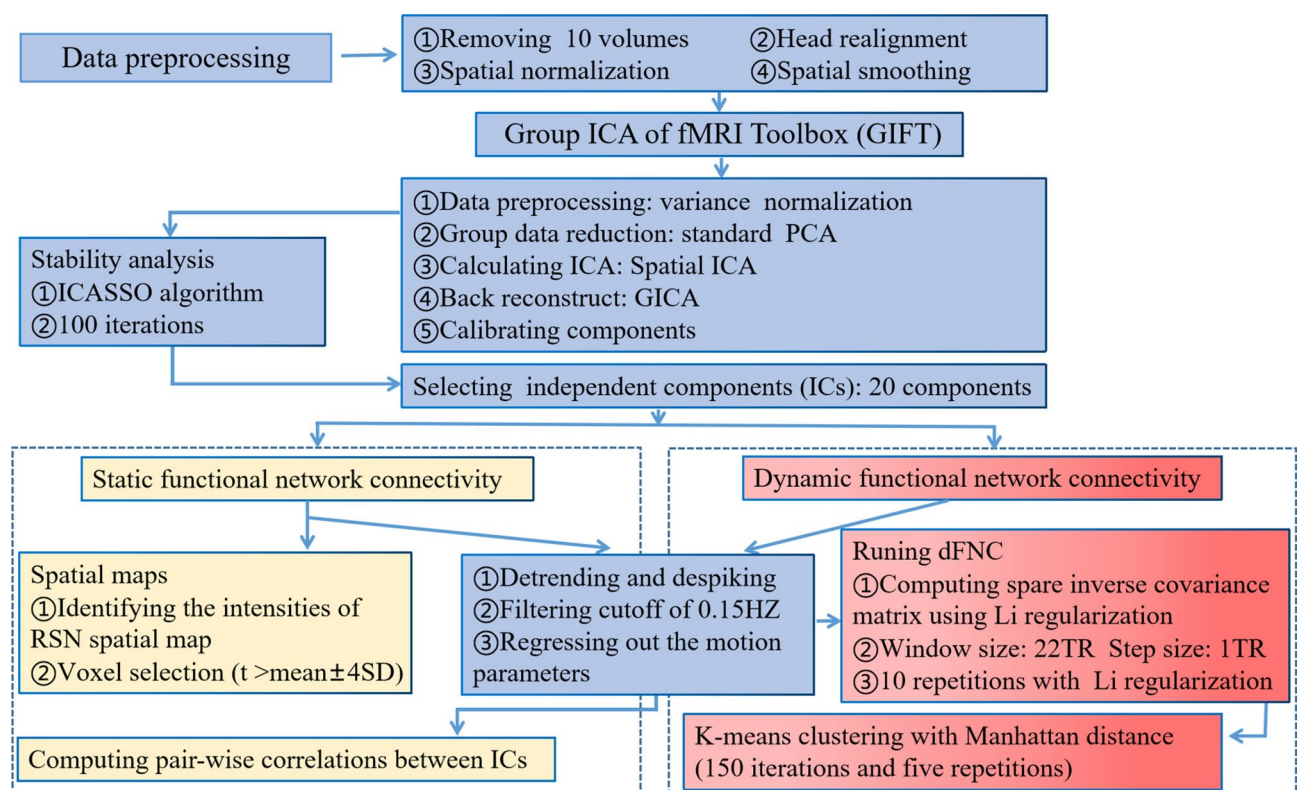

Fig. 1. Schematic illustration of the functional network analyses pipeline. Boxes indicate particular choices made for the data and analysis presented here using the Group ICA of fMRI Toolbox (GIFT). RSN, resting-state network; dFNC, dynamic functional network connectivity; ICA, independent component analysis; PCA, principal component analysis; SD, standard deviation; TR, repetition time.

Static functional networks analysis

We used a multivariate-analysis-of-covariance (MANCOVAN) module in the GIFT toolkit to evaluate the static FC strength of the brain networks. The spatial strength of brain networks was evaluated using spatial maps (SMs). Spatial strength was "thresholded" based on the T-statistic distribution of voxels (such as mean ± 4SD, with SD being the standard deviation) to analyze voxels with strong and consistent activation within individual networks, thereby analyzing the most representative brain regions within each network. For the functional connectivity strength between networks, post-processing was performed on the component time series for each subject using default settings, including using 3dDespike to detrend and remove linear drift, filtering with a fifth-order Butterworth low-pass filter with a high-frequency cutoff of 0.15 Hz, and regressing out six head motion parameters. The resulting time series were Fisher's transformed and pairwise Pearson correlation coefficients, which were calculated to compute the functional connectivity matrix for each patient. Age, sex, and mean FD were continuous variables.

Dynamic functional networks analysis

The analysis was conducted using the sliding window method of the Temporal dFNC module in GIFT v3.0b software. The window width was set to 22TRs (44 s), with a step size of 1TR (2 s)[24,35]. L1 regularization (repeated 10 times) was used to increase the sparsity of the functional connectivity matrix for each window. Therefore, for each participant and each window, a functional connectivity matrix with $\frac{N(N-1)}{2}$ pairs (N, number of ICA components) was obtained, reflecting the temporal changes in functional connectivity among the 20 components. Fisher's Z transformation was then applied to the normalized matrix to obtain Z values and to stabilize the variance for further analysis. During this process, the average FD, sex, and age were regressed simultaneously.

Using the K-means method to conduct cluster analysis of the functional connectivity of brain networks in each time window, repeated patterns of functional connections were extracted to measure the similarity between different time windows using the Manhattan distance (city) as a statistic (150 iterations and five repetitions). The elbow criterion, calculated as the ratio of the within-group to the between-group distance[24], was used to estimate the number of brain FC states, reflecting the different dFNC states of the brain network. The following indicators were used to reflect the temporal features: (1) fractional time, defined as the ratio of the time spent by the subject in each state to the total time; (2) mean dwell time, defined as the time the subject spent in each state; and (3) number of transitions of each subject in different states.

Statistical analysis

We used the Kolmogorov–Smirnov test to assess the normality of the demographic and scale data. Chi-squared, non-parametric, and two-sample t-tests were used to compare differences between the DAI and HCs components based on the data type. We evaluated the differences between the groups in SMs, sFNC, and dFNC using two-sample t-tests, and the results were corrected for multiple comparisons using the false discovery rate (FDR) (P < 0.05). Finally, age, sex, and mean FD were used as control variables, and Spearman's correlation analysis was employed to examine the relationship between altered functional network attributes (network metrics and temporal properties) and clinical variables.

Validation analysis

To test the reliability in our study, we examined whether varying the sliding window length would affect our primary findings. Thus far, no consensus has been reached regarding the optimal length of the sliding window method. Previous research results indicated that a time window of 30–60 s could successfully estimate the dFNC and was not affected by noise[22], and a window length of 44 s resulted in a good balance between estimating connectivity quality and reflecting dynamic attributes[24,36]. Therefore, a dFNC analysis utilizing a window length of 30 TR (60 s) was conducted, in addition to a window length of 22 TR (44 s) with a step size of 1 TR. For consistency, the number of clusters in this step was also set to three. Correlation analysis was performed on the functional connection matrices of the three states.

Results

Demographic and clinical characteristics

As shown in Table 1, there were no statistically significant differences in age (P = 0.98), sex (P = 0.64), or educational (P = 0.97) level between the TBI and HC groups. The clinical scale scores of the DAI group were significantly lower than those of the control group for the Glasgow Comma Score, Disability Rating Scale, Motor Assessment Scale, Hamilton Anxiety Scale, MMSE, and Activities of Daily Living (P < 0.05).

Static functional network analysis

Based on functionality and anatomical characteristics, we created a functional connectivity matrix after identifying 20 from a total of 30 components that were subsequently divided into eight networks. The networks were the DMN, sensorimotor network (SMN), ECN, salience network, VIS, subcortical network (SCN), auditory network (AUD), and CN. Spatial maps of the selected ICs are shown in Fig. 2. Patients with DAI exhibited stronger SMs within the DMN (right anterior cingulate gyrus) and SCN (bilateral caudate nucleus) compared with HCs (P < 0.05, FDR corrected).shown in Fig. 3A. However, no statistically significant difference in inter-network sFNC was found between patients with DAI and HCs (P > 0.05, FDR-corrected) shown in Fig. 3B.

Characteristics	DAI (n = 26)	HC (n = 27)	p-value
Sex (male/female)	18/8	20/7	0.64[a]
Age (years)	38.35 ± 14.59	38.26 ± 13.32	0.98[b]
Education (years)	7.07 ± 3.49	7.11 ± 2.95	0.97[b]
Injury-to-MRI interval (days) (median, range)	24 (2–210)	–	–
Handedness (right), %	100	100	1.0[b]
GCS (Injury)	7.35 ± 4.45	15 ± 0	< 0.01[b]
GCS (Scanning)	13.73 ± 2.38	15 ± 0	0.01[b]
MMSE	19.50 ± 10.48	29.78 ± 0.42	< 0.01[b]
DRS	9.31 ± 6.20	0 ± 0	< 0.01[b]
ABS	32.31 ± 12.60	14 ± 0	< 0.01[b]
MAS	35.88 ± 11.61	47.93 ± 0.27	< 0.01[b]
ADL	33.38 ± 14.54	14.33 ± 0.62	< 0.01[b]
HAMA	10.62 ± 6.89	1.52 ± 1.01	< 0.01[b]

Table 1. Comparison of clinical characteristics among the DAI and HC groups. DAI, diffuse axonal injury; HC, healthy control group; GCS, Glasgow Coma Score; MMSE, Mini-Mental State Examination Scale; DRS, Disability Rating Scale; MAS, Motor Assessment Scale; ABS, Agitated Behavior Scale; ADL, Activities of Daily Living Scale; HAMA, Hamilton Anxiety Scale; M, median; a, chi-square test; b: two-sample t-test; –, no data.
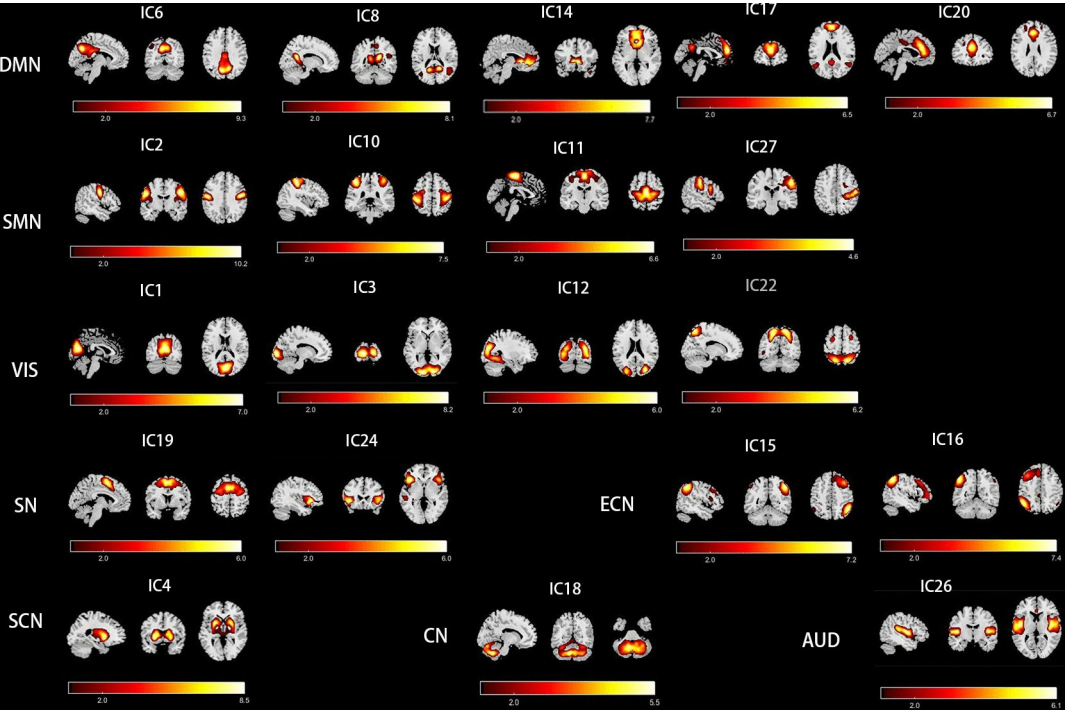

Fig. 2. Spatial maps of 20 independent components representing eight RSNs. The color scale represents the t-values in each component. RSNs, resting-state networks; DMN, default mode network; SMN, sensorimotor network; VIS, visual network; SN, salience network; ECN, executive control network; SCN, subcortical network; CN, cerebellum network; AUD, auditory network.

Dynamic functional network analysis

Differences between groups in dFNC

According to the cluster status estimation results, three recurring functional connectivity states were identified using the k-means clustering method. The corresponding cluster centers of these three states are presented in Fig. 4. Noteworthily, the total percentages of the three states differed in all subjects as follows: state 1, 41%; state 2, 47%; and state 3, 11% (Fig. 4A). State 1 was characterized by relatively moderate connections which were segregated, mainly demonstrating a stronger network FC within the DMN and VIS networks. State 2 exhibited a widespread weaker connectivity of both intra- and inter-networks, whereas state 3 was a tight-connection state and demonstrated stronger connectivity within and between networks, mainly manifested in the SMN and VIS.
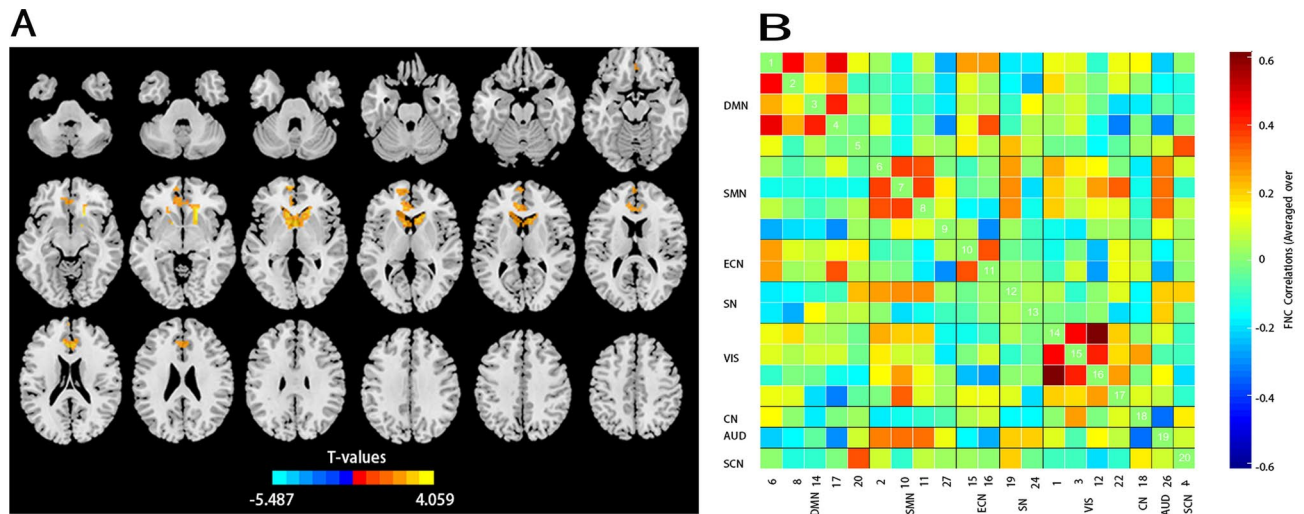
Fig. 3. Results of the voxel-level comparison of RSN maps and sFNC between groups. (**A**) Spatial maps of significant voxels between DAI and HC groups, P < 0.05, FDR corrected. (**B**) sFNC correlations matrix (averaged over subjects). No statistically significant difference in inter-network sFNC was found between groups, P > 0.05, FDR corrected. RSNs, resting-state networks; sFNC, static functional network connectivity; DAI, diffuse axonal injury; HC, health control.

Specifically, the SMN-SCN, SMN-CN, and VIS-SCN connections were negative, whereas the SMN-VIS and SMN-AUD connections were positive and were among the most salient connections in state 3. The present study showed the number of subjects of specific states for each group in Fig. 4B. Patients with DAI showed highest percentage in state 1 (26/26, accounting for 100%), whereas HC group showed highest percentage in state 2 (27/27, accounting for 100%). The percentage is calculated as the ratio of the number of subjects who entered one state to the total number of subjects in each group.

Connection strength analysis of dynamics states
Compared with HCs, the dFNC connection strength revealed that individuals with DAI exhibited mainly increased FC in all states, particularly within the DMN and VIS networks, and state 1 also exhibited aberrant dFNC involving increased inter-network functional connectivity in the VIS-DMN, VIS- executive control network, and VIS- auditory network (Fig. 4C).

Temporal properties of dynamics FC states
As shown in Fig. 5, the between-group difference analysis of dynamic temporal features revealed that in state 1, the fractional time was significantly higher, and the mean dwell time was significantly longer in the DAI group compared to the HC group (P < 0.001, FDR-corrected). In addition, the fractional time was significantly lower and the mean dwell time was also significantly shorter in state 2 in the DAI group compared to the HC group (P < 0.001, FDR-corrected) (Fig. 5A,B). However, we did not find any significant group differences in the number of transitions between the states in the DAI and HC groups (P > 0.05, FDR-corrected) (Fig. 5C).

Correlation analysis
Using the Spearman's rank correlation analysis, we found that the mean dwell time in state 1 was positively associated with MMSE scores in patients with DAI (r = 0.419, P = 0.033) (Fig. 5D).

Validation analysis
By performing validation analysis, we found that our main findings were stable and reproducible when the window length was 22 TR (44 s) and 30 TR (60 s), with a step size of 1 TR. Specifically, altering the sliding window size did not nullify the statistically significant difference in dFNC indicators between the DAI and HC groups. The frequency and dynamic temporal characteristics of the dFNC states (including fractional time and dwell time) and the intergroup differences in dFNC were similar for all subjects (Supplementary Material; Fig. S1, S2); Unfortunately, we found no significant correlations between temporal properties measures and clinical variables. Meanwhile, the data and results of all analytical methods in the study are available in Supplementary Material.

Discussion
Our study revealed the altered sFNC and dFNC features and dynamic temporal properties using combined static and dynamic functional network analyses between patients with DAI and HCs. There were four main findings in patients with DAI: (1) the current study showed stronger intra-network SMs within DMN and SCN, while the inter-network sFNC remained stable with no statistically significant difference after FDR correction; (2) three recurrent dFNC "states" were identified, with stronger network FC within the DMN and VIS networks
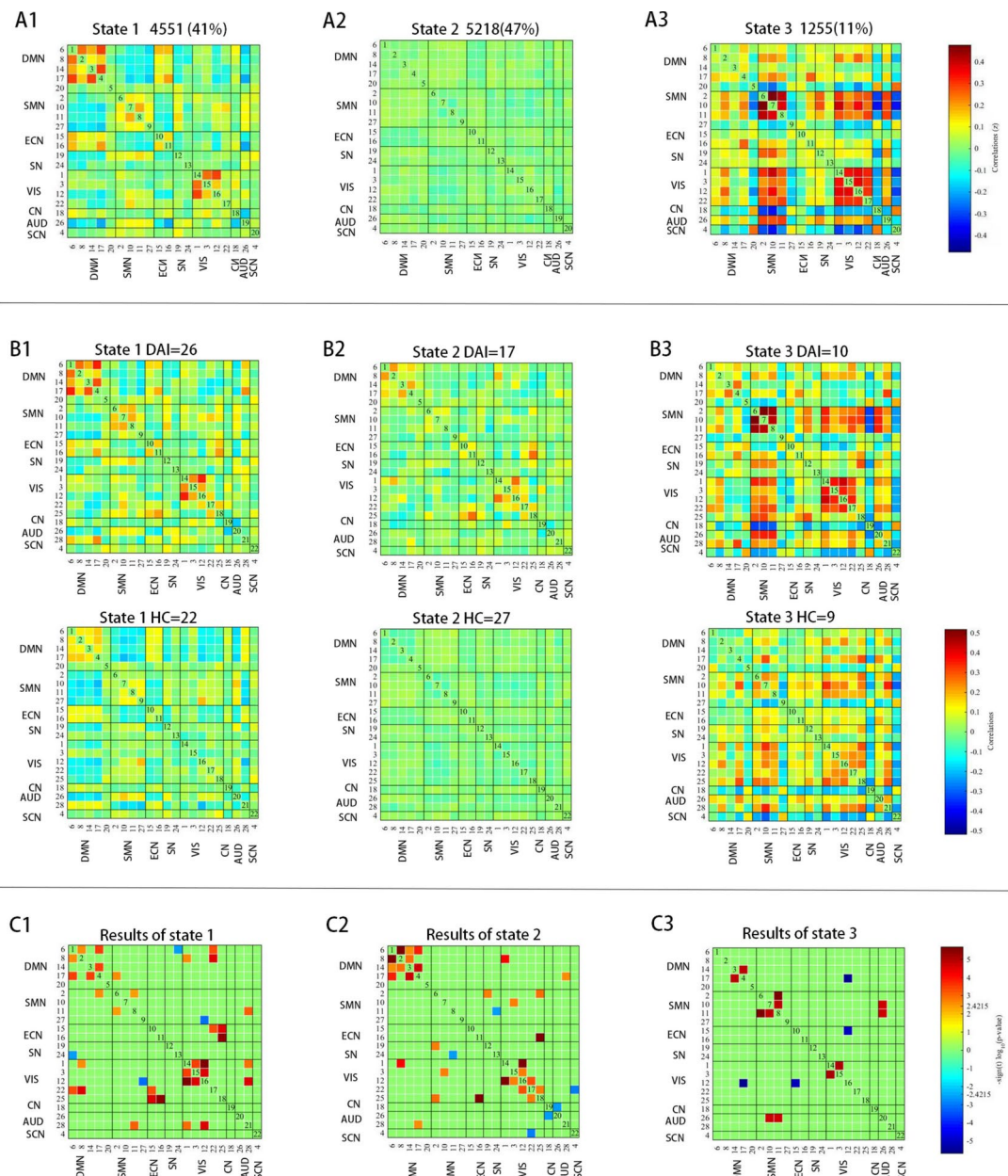
Fig. 4. Results of clustering analysis and significant differences in dFNC between groups. (**A**) Three dFNC states (A1-A3) for all subjects with the total number of occurrences and percentage of total occurrences. (**B**) The specific connectivity state for DAI and HC group, respectively (B1-B3). (**C**) Differences in dFNC between the DAI and HC group. Patients with DAI showed significantly higher dFNC within DMN and VIS compared with HC group in three states (C1-C3), P < 0.05, FDR corrected. dFNC, dynamic functional network connectivity; DAI, diffuse axonal injury; HC, health control; DMN, default mode network; VIS, visual network.

in state 1 occurring most frequently in all patients with DAI (100%); (3) patients with DAI exhibited mostly increased FC strength of dFNC in all states, particularly within the DMN and VIS networks; (4) patients with DAI exhibited higher fractional time and longer mean dwell time in state 1. Moreover, the mean dwell time in state 1 was positively associated with the MMSE score in patients with DAI. The abnormalities in dFNC and temporal properties among patients with DAI might reflect more subtle dynamics changes in the brain and provide distinct complementary individual information different from static FC. The dFNC analysis could enhanced our understanding of the underlying pathophysiological mechanisms in patients with DAI.

The RSNs have become the focus of recent neural physiopathology studies. TBI typically results in axonal injury, which leads to the disruption of coordinated relationships within large-scale functional brain networks[2]. The DMN was the most frequently reported and investigated network. Abnormalities of activation and FC within the DMN, as well as inter-network connectivity have been observed in recent studies, which
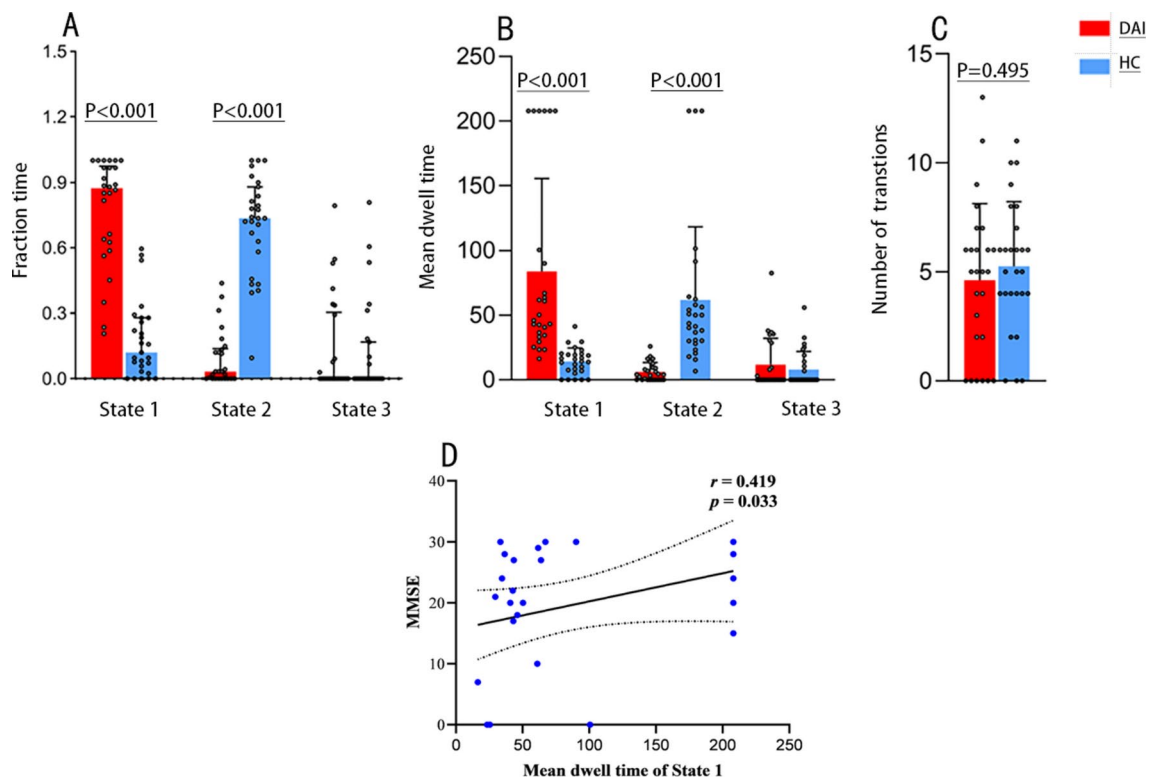
Fig. 5. Between-group comparison of dynamic temporal properties and result of correlation analysis for DAI group. (**A**) Fractional time (i.e., the proportion of the window number per state to the total number of windows) and (**B**) mean dwell time (i.e., the average number of consecutive windows in the same state) are depicted between DAI and the HC groups with significant differences in state 1 and state 2 (p < 0.001, FDR corrected). (**C**) Comparison of the number of transitions (i.e., the total switching times between different states) was not significant difference between groups (P > 0.05, FDR corrected). (**D**) Correlation results between the mean dwell time of state 1 and the MMSE score.

were associated with impaired cognitive and memory domains[37], impaired inhibitory control[38], and visual attention[39]. A previous study found that increased anterior connectivity within the DMN correlated negatively with posttraumatic symptoms[8]. The present study revealed stronger intra-network SMs in the right anterior DMN and the SCN (bilateral caudate nucleus). Previous studies have shown that aberrant activation of the caudate nucleus is linked to deficits in cognitive flexibility[40] and working memory[41] in patients with TBI. These results suggest that abnormal intra-network SMs within SCN and DMN may underlie the common cognitive dysfunction observed in DAI. However, the current results showed no significant between-group difference in sFNC between networks. The finding was supported by a recent study showing no group differences in static FNC survived FDR-correction during post hoc group comparisons between mild to moderate TBI and HCs, including longitudinal effects[42]. Contrarily, some previous studies demonstrated widespread changes in static FNC in the acute stage after mild TBI[6,29]. This potential mechanism may be related to differences in the heterogeneity of TBI and statistical methods, as well as the plasticity of neurons in the recovery phase of the disease. In our study, most patients with DAI are in the subacute phase, which could reflect adaptive processes. Even so, the findings of our study still need to be interpreted cautiously.

In addition, this study explored dynamic FC in patients with DAI, with a specific emphasis on connection strength in dynamic states and temporal characteristics, exhibiting time-varying dynamic features of brain activity. Three recurring states were identified for dFNC in our study, The total percentages of the state1 and state 2 in all subjects was 88%. Meanwhile, the significant differences in temporal properties measures also existed in state 1 and state 2. So, the two divergent brain states may be main dynamic states after DAI. Specifically, State 1 with highest frequency existing in all patients with DAI (26/26, accounting for 100%) was characterized by relatively moderate connection, and mainly demonstrated a stronger network FC within the DMN and VIS networks, which were associated with cognitive impairment[43,44] and high levels of processing deficits[6,45], respectively. The findings might suggest the patients with DAI tend to demonstrate active states in dFNC within the cognitive networks aroused by the brain. State 2 exhibited overall lower connectivity within and between networks, it possibly reflects the baseline state of minimal activity between brain neurons at rest. Results of the dFNC temporal properties demonstrated that patients with DAI exhibited obviously higher fraction time and more dwell time in state 1 rather than state 2 usually exhibited among HCs, suggesting that DAI could cause the transition from the baseline state (state 2) with sparse connectivity to the active state of cognitive networks (state 1) in patients with DAI. Moreover, correlational analysis showed that the mean dwell time in state 1

was positive associated with the MMSE scores in patients with DAI. These findings demonstrate a shift toward more interconnected brain dynamics in patients with DAI showing the distinct increased within-network FC, suggesting that whole-brain connectivity was more segregated and might be associated with cognitive function.

Previous studies with strong evidence have demonstrated that hyperconnectivity is prevalent in individuals with moderate-to-severe TBI, which was hypothesized to represent an adaptive mechanism in regions with the most highly integrated hubs[46–48]. The current study also showed that patients with DAI exhibited mostly increased FC strength of the dFNC in all states compared to HCs, particularly within the DMN and VIS, as well as stronger between-network connections in the VIS-DMN, VIS-ECN, and VIS-AUD (state 1). These findings are referred to as hyperconnectivity which is a common response to neurological disruption and consistent with previous studies[11,49]. Similarly, some fMRI studies demonstrated hyperconnectivity within the DMN in patients with mild TBI[50,51]. Previous study also showed that mild TBI patients demonstrated significantly increased and more variable dynamic cross-network interactions associated with cognitive and behavioral outcomes[30]. Meanwhile, several studies on moderate and severe TBI have demonstrated that enhanced connectivity within sensorimotor and cognitive networks correlated with improved cognitive function[48,52]. The VIS encompasses numerous brain regions susceptible to impact forces. Patients with mild TBI often experience visual dysfunction, which was linked to elevated processing deficits[17,45]. Our findings suggest that increased FC strength of the dFNC within DMN and VIS as well as between VIS can be interpreted as an adaptive response that may mitigate behavioral deficits following DAI[11,42]. This may be accompanied by increases in synaptogenesis, as well as axonal and dendritic sprouting in undamaged axons[53]. Cumulatively, the Hyperconnectivity within vital networks may yield valuable insights into the potential adaptive mechanism in response to structural damage in the subacute phase of disease after DAI, leading to enhanced synchrony.

Nonetheless, hyperconnectivity should not be indiscriminately interpreted as supportive of the compensation hypothesis which may be likely to be metabolically costly[53]. Excessive and continuous augmentation of network connectivity may not always yield long-term benefits. For example, increased demand on cognitive control resources permits task continued completion but with reduced efficiency and slowed information processing[49]. This pattern of hyperconnectivity is negatively associated with task performance and positively associated with severity score[54]. Previous study demonstrated that patients with moderate to severe TBI who showed higher connectivity degree displayed lower switching performance and more severe head injury[55].

The current study has several limitations. First, considering TBI heterogeneity (severity, course, type of injury), 29 patients with larger local hemorrhages and 2 patients diagnosed with mild TBI were excluded to examine among the 57 patients with DAI. Therefore, the final sample size was relatively small. In the future, we will continue to recruit patients with DAI to conduct larger-sample studies. Second, we used ICA to extract resting-state networks, ignoring topographic idiosyncrasies which might reflect individual differences between DAI and HC groups affecting FNC. Hyperalignment[56,57] and individualized parcellations[58,59] were deemed to be used to resolve topographic idiosyncrasies which can improve prediction performance. We will emphasize individual differences in functional organization[56] and addresses the bias and achieves more accurate connectivity estimates[60] in future work. Additionally, the results of dFNC showed hyperconnectivity in current study, which could reflect adaptive processes. However, there is no consensus on the functional utility of hyperconnectivity, the findings of our study still need to be interpreted cautiously. In order to determine the specific function of hyperconnectivity in brain injury, it is necessary to study its evolution on different temporal and spatial scales, focusing on identifying the consequences of symptoms and recovery, and further longitudinal analyses are required to investigate the predictive value of dynamic functional connections.

Conclusion

This study explored the static and dynamic FNC patterns in patients with DAI. Compared to HCs, patients with DAI showed aberrant dFNC and altered temporal properties, whereas there was no significant difference in inter-network sFNC. The findings showed that dFNC and temporal properties might provide unique complementary information distinct from static FC and insights into the underlying pathophysiological mechanisms of patients with DAI, and may serve as potential biomarkers for diagnosing DAI and cognitive deficits after injury.

Data availability

The raw data supporting the conclusions of this article will be provided by the corresponding author without reservation.

References

1. Dewan, M. C. et al. Estimating the global incidence of traumatic brain injury. *J. Neueosurg.* **130**, 1080–1097 (2018).
2. Sharp, D. J., Scott, G. & Leech, R. Network dysfunction after traumatic brain injury. *Nat. Rev. Neurol.* **10**, 156–166 (2014).
3. Jolly, A. E. et al. Detecting axonal injury in individual patients after traumatic brain injury. *Brain* **144**, 92–113 (2021).
4. Benjamini, D. et al. Diffuse axonal injury has a characteristic multidimensional MRI signature in the human brain. *Brain* **144**, 800–816 (2021).
5. Smith, L. et al. Advanced neuroimaging in traumatic brain injury: An overview. *Neurosurg. Focus* **47**, E17 (2019).
6. Li, F. et al. Disrupted functional network connectivity predicts cognitive impairment after acute mild traumatic brain injury. *CNS Neurosci. Ther.* **26**, 1083–1091 (2020).
7. Lampros, M. et al. The role of novel imaging and biofluid biomarkers in traumatic axonal injury: An updated review. *Biomedicines* **11**, 2312 (2023).
8. Zhou, Y. et al. Default-mode network disruption in mild traumatic brain injury. *Radiology* **265**, 882–892 (2012).

9. Lu, L. et al. Functional connectivity dysfunction of insular subdivisions in cognitive impairment after acute mild traumatic brain injury. *Brain Imaging Behav.* **14**, 941–948 (2020).
10. Woodrow, R. E. et al. Acute thalamic connectivity precedes chronic post-concussive symptoms in mild traumatic brain injury. *Brain* **146**, 3484–3499 (2023).
11. Morelli, N. et al. Resting state functional connectivity responses post-mild traumatic brain injury: a systematic review. *Brain Inj.* **35**, 1326–1337 (2021).
12. Vasa, F. et al. Conservative and disruptive modes of adolescent change in human brain functional connectivity. *Proc. Natl. Acad. Sci. U S A* **117**, 3248–3253 (2020).
13. Mayer, A. R., Mannell, M. V., Ling, J., Gasparovic, C. & Yeo, R. A. Functional connectivity in mild traumatic brain injury. *Hum Brain Mapp.* **32**, 1825–1832 (2011).
14. Xu, Z. et al. Disrupted functional connectivity of the striatum in patients with diffuse axonal injury: A resting-state functional MRI study. *Neuroreport* **34**, 792–800 (2023).
15. Wang, Y. et al. Functional plasticity in lateral hypothalamus and its prediction of cognitive impairment in patients with diffuse axonal injury: evidence from a resting-state functional connectivity study. *Neuroreport* **32**, 588–595 (2021).
16. Li, J, et al. Detection of functional homotopy in traumatic axonal injury. *Eur. Radiol.* **27**, 325–335 (2017).
17. Li, F. et al. Altered static and dynamic functional network connectivity in post-traumatic headache. *J. Headache Pain* **22**, 137 (2021).
18. Dretsch, M. N. et al. Strength and temporal variance of the default mode network to investigate chronic mild traumatic brain injury in service members with psychological trauma. *J. Exp. Neurosci.* **13**, 2082133138 (2019).
19. Vergara, V. M., Mayer, A. R., Damaraju, E., Kiehl, K. A. & Calhoun, V. Detection of mild traumatic brain injury by machine learning classification using resting state functional network connectivity and fractional anisotropy. *J. Neurotrauma* **34**, 1045–1053 (2017).
20. Ke, J, et al. Typhoon-related post-traumatic stress disorder and trauma might lead to functional integration abnormalities in intra- and inter-resting state networks: A resting-state Fmri independent component analysis. *Cell Physiol. Biochem.* **48**, 99–110 (2018).
21. Jalilianhasanpour, R. et al. Dynamic brain connectivity in resting state functional MR imaging. *Neuroimaging Clin. N Am.* **31**, 81–92 (2021).
22. Preti, M. G., Bolton, T. A. & Van De Ville, D. The dynamic functional connectome: State-of-the-art and perspectives. *Neuroimage* **160**, 41–54 (2017).
23. Lurie, D. J. et al. Questions and controversies in the study of time-varying functional connectivity in resting fMRI. *Netw. Neurosci.* **4**, 30–69 (2020).
24. Allen, E. A. et al. Tracking whole-brain connectivity dynamics in the resting state. *Cereb. Cortex* **24**, 663–676 (2014).
25. Gan, C. et al. Dynamic functional connectivity reveals hyper-connected pattern and abnormal variability in freezing of gait of Parkinson's disease. *Neurobiol. Dis.* **185**, 106265 (2023).
26. Wang, Y. et al. Temporal and topological properties of dynamic networks reflect disability in patients with neuromyelitis optica spectrum disorders. *Sci. Rep.* **14**, 4199 (2024).
27. Hyatt, C. J. et al. Atypical dynamic functional network connectivity state engagement during social-emotional processing in schizophrenia and autism. *Cereb. Cortex* **32**, 3406–3422 (2022).
28. Vergara, V. M., Mayer, A. R., Kiehl, K. A. & Calhoun, V. D. Dynamic functional network connectivity discriminates mild traumatic brain injury through machine learning. *Neuroimage Clin.* **19**, 30–37 (2018).
29. Lu, L. et al. Aberrant static and dynamic functional network connectivity in acute mild traumatic brain injury with cognitive impairment. *Clin. Neuroradiol.* **32**, 205–214 (2022).
30. Li, X. et al. Brain dynamics in triple-network interactions and its relation to multiple cognitive impairments in mild traumatic brain injury. *Cereb. Cortex* **33**, 6620–6632 (2023).
31. Mayer, A. R. et al. Static and dynamic intrinsic connectivity following mild traumatic brain injury. *J. Neurotrauma* **32**, 1046–1055 (2015).
32. Hutchison, R. M. et al. Dynamic functional connectivity: Promise, issues, and interpretations. *Neuroimage* **80**, 360–378 (2013).
33. Allen, E. A. et al. A baseline for the multivariate comparison of resting-state networks. *Front. Syst. Neurosci.* **5**, 2 (2011).
34. Wang, Y. et al. Male and female are not the same: A multicenter study of static and dynamic functional connectivity in relapse-remitting multiple sclerosis in China. *Front. Immunol.* **14**, 1216310 (2023).
35. Dai, Y. et al. Altered dynamic functional connectivity associates with post-traumatic stress disorder. *Brain Imaging Behav.* **17**, 294–305 (2023).
36. Fiorenzato, E. et al. Dynamic functional connectivity changes associated with dementia in Parkinson's disease. *Brain* **142**, 2860–2872 (2019).
37. Abdul, R. M. et al. Alteration in the functional organization of the default mode network following closed non-severe traumatic brain injury. *Front. Neurosci.* **16**, 833320 (2022).
38. Bonnelle, V. et al. Salience network integrity predicts default mode network function after traumatic brain injury. *Proc. Natl. Acad. Sci. U S A* **109**, 4690–4695 (2012).
39. Kim, Y. H. et al. Plasticity of the attentional network after brain injury and cognitive rehabilitation. *Neurorehabil. Neural Repair* **23**, 468–477 (2009).
40. Pauli, W. M., O'Reilly, R. C., Yarkoni, T. & Wager, T. D. Regional specialization within the human striatum for diverse psychological functions. *Proc. Natl. Acad. Sci. U S A* **113**, 1907–1912 (2016).
41. Newsome, M. R. et al. Disruption of caudate working memory activation in chronic blast-related traumatic brain injury. *Neuroimage Clin.* **8**, 543–553 (2015).
42. van der Horn, H. J. et al. Functional outcome is tied to dynamic brain states after mild to moderate traumatic brain injury. *Hum. Brain Mapp.* **41**, 617–631 (2020).
43. Zhu, D. C. et al. A potential biomarker in sports-related concussion: Brain functional connectivity alteration of the default-mode network measured with longitudinal resting-state fMRI over thirty days. *J. Neurotrauma* **32**, 327–341 (2015).
44. Dumkrieger, G., Chong, C. D., Ross, K., Berisha, V. & Schwedt, T. J. Static and dynamic functional connectivity differences between migraine and persistent post-traumatic headache: A resting-state magnetic resonance imaging study. *Cephalalgia* **39**, 1366–1381 (2019).
45. Palacios, E. M. et al. Resting-state functional connectivity alterations associated with six-month outcomes in mild traumatic brain injury. *J. Neurotrauma* **34**, 1546–1557 (2017).
46. Hillary, F. G., Grafman J. H., Injured Brains and Adaptive Networks: The Benefits and Costs of Hyperconnectivity. Trends Cogn Sci. **21**, 385–401 (2017)
47. Hillary, F. G. et al. The rich get richer: Brain injury elicits hyperconnectivity in core subnetworks. *PLoS One* **9**, e104021 (2014).
48. Roy, A. et al. The evolution of cost-efficiency in neural networks during recovery from traumatic brain injury. *PLoS One* **12**, e170541 (2017).
49. Hillary, F. G. et al. Hyperconnectivity is a fundamental response to neurological disruption. *Neuropsychology* **29**, 59–75 (2015).
50. Nathan, D. E. et al. Exploring variations in functional connectivity of the resting state default mode network in mild traumatic brain injury. *Brain Connect.* **5**, 102–114 (2015).
51. van der Horn, H. J. et al. The default mode network as a biomarker of persistent complaints after mild traumatic brain injury: A longitudinal functional magnetic resonance imaging study. *J. Neurotrauma* **34**, 3262–3269 (2017).

52. Shumskaya, E., van Gerven, M. A., Norris, D. G., Vos, P. E. & Kessels, R. P. Abnormal connectivity in the sensorimotor network predicts attention deficits in traumatic brain injury. *Exp. Brain Res.* **235**, 799–807 (2017).
53. Fornito, A., Zalesky, A. & Breakspear, M. The connectomics of brain disorders. *Nat. Rev. Neurosci.* **16**, 159–172 (2015).
54. Caeyenberghs, K. et al. Mapping the functional connectome in traumatic brain injury: What can graph metrics tell us?. *Neuroimage* **160**, 113–123 (2017).
55. Caeyenberghs, K. et al. Graph analysis of functional brain networks for cognitive control of action in traumatic brain injury. *Brain* **135**, 1293 (2012).
56. Feilong, M., Guntupalli, J. S. & Haxby, J. V. The neural basis of intelligence in fine-grained cortical topographies. *Elife* **10**, e64058 (2021).
57. Haxby, J. V., Guntupalli, J. S., Nastase, S. A. & Feilong, M. Hyperalignment: Modeling shared information encoded in idiosyncratic cortical topographies. *Elife* **9**, e56601 (2020).
58. Kong, R. et al. Individual-specific areal-level parcellations improve functional connectivity prediction of behavior. *Cereb. Cortex* **31**, 4477–4500 (2021).
59. Farahibozorg, S. R. et al. Hierarchical modelling of functional brain networks in population and individuals from big fMRI data. *Neuroimage* **243**, 118513 (2021).
60. Bijsterbosch, J. D., Beckmann, C. F., Woolrich, M. W., Smith, S. M. & Harrison, S. J. The relationship between spatial configuration and functional connectivity of brain regions revisited. *Elife* **8**, e44890 (2019).

Acknowledgements

Author contributions

X.Z. guided and designed the MRI experiments. Y.W. analyzed the resting-state fMRI data and performed the statistical analysis. J.L. ordered the results and wrote the manuscript. Y.W., Y.O., W.S., J.Z., X.Z., Z.X., L.L., and J.X. collected the resting-state fMRI and clinical data. X.Z. and F.Z. reviewed and revised the manuscript. All the authors contributed to the manuscript and approved the submitted version.

Funding

Declarations

Competing interests

The authors declare no competing interests.

Additional information

Supplementary Information The online version contains supplementary material available at https://doi.org/10.1038/s41598-024-79052-4.

Correspondence and requests for materials should be addressed to X.Z.

Reprints and permissions information is available at www.nature.com/reprints.

Publisher's note Springer Nature remains neutral with regard to jurisdictional claims in published maps and institutional affiliations.